large cracks (named as main cracks to distinguish them from other cracks) on the ground surface located on the each side of the tunnel axis respectively. Other cracks were almost located within the region between the two main cracks. The distance from left main crack to the tunnel axis is about 31cm; the distance from right main crack to the tunnel axis is about 24 cm.

35 minutes after watering, the water flow turned into debris flow. Due to the erosion of the surrounding rocks, the cracks inside and on the surface of the ground developed quickly. The two main cracks became deeper and wider, and several small cracks occurred on the ground between the two main cracks. The settlement of the region between the two main cracks developed more quickly than that out of this region. The cavern became larger and all the LVDTs inside the strata were dropped down and out of work.

The obvious debris flow and serious collapse lasted for about 25 minutes; then, the flow became smaller and collapse stopped. 3 hours later after watering, no water flow or debris flow could be observed. Figure 5(b) gives the collapse profile and cracks of the model at that time. The cavern above the original tunnel developed upwards and its top face was very near the ground surface. The cavern's diameter is 27 cm, and the distance between the top face of the cavern and the ground surface is 14 cm. The biggest width of the main cracks is 0.4 cm, and the biggest depth of the main cracks is 12 cm.

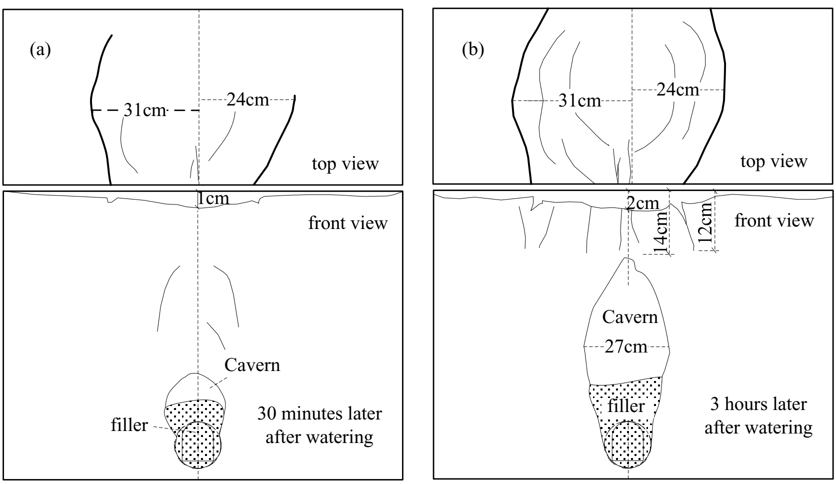

Figure 5. Sketch of the model 30 minutes and 3 hours later after watering

The damage phenomena after watering are very similar to those which took place in the Beigang Tunnel; therefore, the collapse phenomena of the Beigang tunnel were reproduced in the model to some extent.

Based on the collapse characteristics observed in the model test, besides the weak surrounding rock mass, large water infiltration may be the main factor resulting in the collapse of the Beigang Tunnel. The water flow carried out a lot of soil particles, and the surrounding rock mass became loose and full of cracks. Due to larger void ratio and internal cracks, the seepage velocity increased and the problem of flow became more serious. The strength of the surrounding rock mass lessened as a result of mass loss, so the tunnel collapsed.

CONCLUSION

Taking the Beigang tunnel as a prototype, model tests were conducted to investigate the deformation, cracks and collapse pattern of surrounding rock mass when tunneling in weak rock with high water content. Similar damage phenomena of the Beigang tunnel were reproduced in the model test. The following conclusions can be drawn from the analysis:

1) Water infiltration, which induced soil erosion and decreased the strength of the surrounding soils, was mainly responsible for the tunnel's collapse.

2) The distribution of surface settlements at the transverse section before surface cracks appeared can be described well by Peck's Normal Probability Curve.

3) Two main cracks, the two deepest and widest cracks, appearing on the ground surface in the early stages of collapse were located on the each side of the tunnel axis respectively. The settlements and cracks on ground surface developed mainly in the region between the two largest cracks. During tunneling, this region should be carefully monitored, and once the cracks occur on the ground, proper measures must be taken in order to control the collapse of the tunnel.

ACKNOWLEDGEMENTS

This research was financially supported by the National Basic Research Program of China, No. 2010CB732103.

REFERENCES

Hou, J. H. (2009). "Treatment of the collapse of Gangcheng tunnel of Taiyuan." *Journal of Railway Engineering Society*, 10, 74-78.

Jia, J. B., Jiao, C. and Fan P. (2006). "Analysis on ground surface deformation induced by undercutting under shallow overburden in Tianjin Metro." *Tunnel Construction*, 1, 18-20.

Lee, C. J., Wu, B. R. and Chiou, S. Y. (1999). "Soil movements around a tunnel in soft soils." *Proc. Natl. Sci. Counc. ROC.* 2, 235-247.

O'Reilly, M. P. and New, B. M. (1982) "Settlements above tunnels in the United Kingdom-their magnitude and prediction." *Tunneling*, 179-185.

Peck, R. B. (1969). "Deep excavations and tunneling in soft ground." *Proceedings of the 7th International Conference on Soil Mechanics and Foundation Engineering, state-of-the-art Volume*, 225-290. Mexico City, Mexico.

Qi, H. T., Gao, B. and Ma, J. L. (2006). "Centrifugal model test for ground surface subsidence caused by metro tunneling in saturated soft clay strata." *Journal of Southwest Jiaotong University*, 2, 184-189.

Sterpi, D. and Cividini, A. (2004). “A physical and numerical investigation on the stability of shallow tunnels in strain softening media.” *Rock Mechanics and Rock Engineering*, 4, 277- 298.
Yuan Q. (2003). “Analysis of the reason and control of ground settlement of subway at Guangzhou Subway No. 2 line Kecun contact line fork.” *Journal of Shijiazhuang Railway Institute*, 7, 19-22.
Zhou, X. W. and Pu, J. L. (2002). “Centrifuge model test on ground settlement induced by tunneling in sandy soil.” *Soil Mechanics*, 5, 559-563.
Zhou, Y. F. (2007). “The discussion of construction method on Beigang tunnel crossing-over weak-fracture zone.” *Shanxi Architecture.* 19, 313-314.

Application of Story Isolation Technique in the Seismic Reduction of Integrated Building-Bridge Station

Guo, W.[1], Yu, Z.[2] and Zhang, H.S.[3]

[1] Lecturer, School of Civil Engineering, Central South University, Hunan 410075, China; email: wei.guo.86@gmail.com
[2] Professor, School of Civil Engineering, Central South University, Hunan 410075, China; email: zhwyu@mail.csu.edu.cn
[3] Postgraduate student, School of Civil Engineering, Central South University, Hunan 410075, China; email: zhanghuashuai222@163.com

ABSTRACT

As a novel structure, the integrated building-bridge station has appeared in the high speed railway construction of China, which is of great significant to ensure the seismic safety of the new structure in an earthquake. Meanwhile, the isolation technique which is an important passive control strategy has also been widely used in both buildings and bridges. Based on these, an intensive study of the story isolation technique is carried out in this paper which is to investigate the isolation technique's feasibility and effect on the integrated building-bridge station. Firstly, given the special characteristics of structure and isolation devices which are usually installed on the connection positions between the building and bridge, the numerical model is established considering the dynamic coupling effect. As earthquake ground motion is practically a random process, an accurate and efficient stochastic expression is derived based on the pseudo-excitation method and complex mode technique. Then a rational and effective optimization strategy is proposed to achieve the appropriate setting of the isolation devices. Finally, a numerical example is given to investigate the story isolation technique's application in the integrated building-bridge station by utilizing the stochastic analysis method and optimization strategy proposed in this paper.

INTRODUCTION

Regarded as an important public structure and transportation hub, the safety issue of the integrated building-bridge station in an earthquake is of great significance, and it is necessary to perform seismic control design for such structures. Currently the most common and widespread application of vibration control strategy in seismic control is isolation design, which includes base isolation and story isolation. The isolation technique is usually applied to lower buildings, which has been proved to be very effective by the scholars all over the world in their research (Zhou, 1997; Liu, 2004; Skinner and Robinson, 1993; Naeim and Kelly, 1993; Kelly, 1997) which has been developed systematically, and some correlative research achievements have already been applied to engineering. Therefore, for the integrated building-bridge station, how to introduce the isolation technique in construction and achieve the appropriate parameter setting to reduce vibration in an earthquake has considerable significance. Liu et al. (2008) pointed out that it is impossible to achieve cooperative vibration control by installing the appropriate set isolation devices on the connection part of building and bridge in their research work about the seismic design of integrated building-bridge stations based on the translational single-DOF model and time history analysis, and. Fang (2004) studied the isolation application in the sub-frame and mega-frame structures. His theoretical model is similar to the integrated building-bridge station.

Based on the statement above, the multi-DOF numerical model of the integrated building-bridge station which takes into account the coupling effect between the building and bridge is established in this paper. Considering the earthquake ground motion as a random process, the accurate and efficient stochastic calculation expression is also derived based on the complex mode theory and pseudo excitation method (Lin and Zhang, 2004). In fact the parameter optimization of isolation devices applied in the integrated building-bridge station is a multi-objective problem, so the parameter field method is introduced in this paper to appropriately determine the optimal setting of isolation devices and corresponding vibration reduction effect. Finally, a numerical example is given to investigate the working mechanism and the damping effect of the story isolation technology applied in the integrated building-bridge station.

STORY ISOLATION MODEL

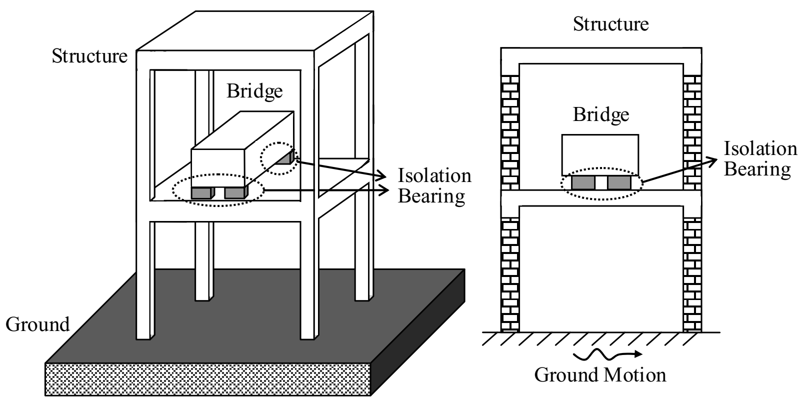

(a) actual entity model (b) simple translational model

Figure 1. Schematic diagram of integrated building-bridge station with isolation devices

Figure 1 gives the schematic diagram of setting isolation devices in the bottom of the bridge structure, in which Figure 1(a) describes the entity model and Figure 1(b) is an simplified model of the integrated building-bridge station. Based on such a model, the dynamic equilibrium equation of multi-DOF model can be established as follows:

$$\boldsymbol{M}_s\ddot{\boldsymbol{U}}_s+\boldsymbol{C}_s\dot{\boldsymbol{U}}_s+\boldsymbol{K}_s\boldsymbol{U}_s=-\boldsymbol{M}_s\boldsymbol{E}_s\ddot{u}_g+\boldsymbol{E}_bF_b\,,\ \ m_b\ddot{u}_b+F_b^{'}=-m_b\ddot{u}_g \tag{1a,b}$$

in which $\boldsymbol{M}_s$, $\boldsymbol{C}_s$ and $\boldsymbol{K}_s$ are the mass, damping and stiffness matrices of n DOF building respectively; $\boldsymbol{U}_s=[u_{s1},u_{s2},\ldots,u_{sn}]^T$ is the displacement vector of the building relative to the ground; m_b is the mass of bridge; u_b is the displacement vector of the bridge relative to the building; $\ddot{u}_g$ is the acceleration of the ground; $\boldsymbol{E}_s$ represents the position vector of the earthquake force; $\boldsymbol{E}_b$ represents the position vector of the force F_b; F_b is the external force on the building provided by the bridge; $-F_b^{'}$ is the external force on the bridge provided by the building; $F_b=F_b^{'}=c_b\dot{u}_b+k_bu_b$; $c_b=2m_b\omega_b\xi_b$, $k_b=m_b\omega_b^2$ are the damping coefficient and stiffness coefficient of the isolation devices, respectively; ω_b and ξ_b are the circular frequency and damping ratio, respectively. Based on equation (1), the dynamic equilibrium equation of integrated building-bridge station can be obtained:

$$\boldsymbol{M}\ddot{\boldsymbol{U}}+\boldsymbol{C}\dot{\boldsymbol{U}}+\boldsymbol{K}\boldsymbol{U}=-\boldsymbol{M}\boldsymbol{E}\ddot{u}_g \tag{2}$$

in which, $\boldsymbol{M}=\begin{bmatrix}\boldsymbol{M}_s & \boldsymbol{0}_{n\times1}\\ \boldsymbol{0}_{n\times1} & m_b\end{bmatrix}$, $\boldsymbol{C}=\begin{bmatrix}\boldsymbol{C}_s+\boldsymbol{C}_s^{(b)} & \boldsymbol{C}_{sb}\\ \boldsymbol{C}_{bs} & c_b\end{bmatrix}$ and $\boldsymbol{K}=\begin{bmatrix}\boldsymbol{K}_s+\boldsymbol{K}_s^{(b)} & \boldsymbol{K}_{sb}\\ \boldsymbol{K}_{bs} & k_b\end{bmatrix}$ are the mass, damping and stiffness matrices of the integrated building-bridge station respectively, and the total DOF of the structure is $n+1$; $\boldsymbol{C}_s$, $\boldsymbol{K}_s$, c_b and k_b have been defined above; $\boldsymbol{C}_{sb}$, $\boldsymbol{C}_{bs}$, $\boldsymbol{K}_{sb}$ and $\boldsymbol{K}_{bs}$ are the coupled damping and stiffness matrices associated with both the building and the bridge; $\boldsymbol{C}_s^{(b)}$ and $\boldsymbol{K}_s^{(b)}$ represent the force on the building reacted from the bridge; $\boldsymbol{U}=[\boldsymbol{U}_s^T,u_b]^T$ is the displacement vector relative to the ground; $\boldsymbol{E}=[\boldsymbol{E}_s^T,1]^T$ is the vector of earthquake force position.

Since the isolation devices are set on the bottom of bridge, the integrated building-bridge station has non-proportional damping characteristic. So, in order to realize decoupling calculation the state vector method and complex mode theory are generally adopted. Firstly define the state vector:

$$\bar{\boldsymbol{U}}=\begin{bmatrix}\dot{\boldsymbol{U}} & \boldsymbol{U}\end{bmatrix}^T \tag{3}$$

Introduce the equation $\boldsymbol{M}\dot{\boldsymbol{U}}-\boldsymbol{M}\dot{\boldsymbol{U}}=\boldsymbol{0}$; the state equation can be established as follows:

$$\boldsymbol{A}\dot{\bar{\boldsymbol{U}}}+\boldsymbol{B}\bar{\boldsymbol{U}}=-\boldsymbol{A}\bar{\boldsymbol{E}}\ddot{u}_g \tag{4}$$

in which $\boldsymbol{A}=\begin{bmatrix}\boldsymbol{0} & \boldsymbol{M}\\ \boldsymbol{M} & \boldsymbol{C}\end{bmatrix}$, $\boldsymbol{B}=\begin{bmatrix}-\boldsymbol{M} & \boldsymbol{0}\\ \boldsymbol{0} & \boldsymbol{K}\end{bmatrix}$, $\bar{\boldsymbol{E}}=\begin{bmatrix}\boldsymbol{E}\\ \boldsymbol{0}_{(n+1)\times1}\end{bmatrix}$. For the under-damped model described by equation (4), there exists $n+1$ groups of eigenvalue and eigenvector, which are conjugate with each other in one certain group. Then the following equation can be given:

$$\boldsymbol{B}\boldsymbol{\Phi}_i=-\eta_i\boldsymbol{A}\boldsymbol{\Phi}_i \tag{5}$$

in which $\boldsymbol{\Phi}_i=\begin{bmatrix}\eta_i\boldsymbol{\varphi}_i\\ \boldsymbol{\varphi}_i\end{bmatrix}$, $\boldsymbol{\varphi}_i=\boldsymbol{\varphi}_{iR}+r\boldsymbol{\varphi}_{iI}$, $\eta_i=-\eta_{iR}+r\eta_{iI}=-\xi_i\omega_i+r\omega_i\sqrt{1-\xi_i^2}$, $r=\sqrt{-1}$, $i=1\sim n+1$. There exist generalized orthogonality relationship for different eigenvectors, and utilizing the relationship the circular frequency ω_i and damping ration ξ_i are:

$$\omega_i^2 = \frac{\left(\boldsymbol{\varphi}_i^*\right)^T \boldsymbol{K}\boldsymbol{\varphi}_i}{\left(\boldsymbol{\varphi}_i^*\right)^T \boldsymbol{M}\boldsymbol{\varphi}_i}\ ,\ 2\xi_i\omega_i = \frac{\left(\boldsymbol{\varphi}_i^*\right)^T \boldsymbol{C}\boldsymbol{\varphi}_i}{\left(\boldsymbol{\varphi}_i^*\right)^T \boldsymbol{M}\boldsymbol{\varphi}_i} \tag{6}$$

in which superscripts $*$ denote the conjugate complex. Using the $2(n+1)$ complete orthonormal eigenvectors, the response of the integrated building-bridge station is expressed as:

$$\boldsymbol{U} = \sum_{i=1}^{2(n+1)} \boldsymbol{\Phi}_i Q_i \tag{7}$$

in which Q_i is the number i generalized displacement response of the structure. Substituting equation (7) into equation (4), and pre-multiplying by $\boldsymbol{\Phi}_i^T$, one can get:

$$\dot{Q}_i - \eta_i Q_i = -\mu_i \ddot{u}_g \tag{8}$$

in which $\eta_i = -\dfrac{\boldsymbol{\Phi}_i^T \boldsymbol{B}\boldsymbol{\Phi}_i}{\boldsymbol{\Phi}_i^T \boldsymbol{A}\boldsymbol{\Phi}_i}$, $\mu_i = \dfrac{\boldsymbol{\Phi}_i^T \boldsymbol{R}\bar{\boldsymbol{E}}}{\boldsymbol{\Phi}_i^T \boldsymbol{A}\boldsymbol{\Phi}_i}$. Meanwhile, define q_i as the response of the following model:

$$\ddot{q}_i + 2\xi_i\omega_i\dot{q}_i + \omega_i^2 q_i = -\ddot{u}_g \tag{9}$$

As is shows in Zhou and Yu (2006), by orthogonality of modes and matrix transformation the structural response can easily be obtained:

$$\boldsymbol{U} = \sum_{i=1}^{n+1}\left[\boldsymbol{X}_i q_i + \boldsymbol{Y}_i \dot{q}_i\right] \tag{10}$$

in which , $\boldsymbol{X}_i = \dfrac{2}{a_i^2 + b_i^2}\left[\left(\xi_i p_i + \sqrt{1-\xi_i^2}\, w_i\right)\boldsymbol{\varphi}_{iR} + \left(\xi_i w_i - \sqrt{1-\xi_i^2}\, p_i\right)\boldsymbol{\varphi}_{iI}\right]\omega_i$,

$\boldsymbol{Y}_i = \dfrac{2}{a_i^2 + b_i^2}\left(p_i\boldsymbol{\varphi}_{iR} + w_i\boldsymbol{\varphi}_{iI}\right)$, $a_i = -2\eta_{iR}\left(\boldsymbol{\varphi}_{iR}^T\boldsymbol{M}\boldsymbol{\varphi}_{iR} - \boldsymbol{\varphi}_{iI}^T\boldsymbol{M}\boldsymbol{\varphi}_{iI}\right) - 4\eta_{iI}\boldsymbol{\varphi}_{iR}^T\boldsymbol{M}\boldsymbol{\varphi}_{iI} + \boldsymbol{\varphi}_{iR}^T\boldsymbol{C}\boldsymbol{\varphi}_{iR} - \boldsymbol{\varphi}_{iI}^T\boldsymbol{C}\boldsymbol{\varphi}_{iI}$,

$b_i = 2\eta_{iI}\left(\boldsymbol{\varphi}_{iR}^T\boldsymbol{M}\boldsymbol{\varphi}_{iR} - \boldsymbol{\varphi}_{iI}^T\boldsymbol{M}\boldsymbol{\varphi}_{iI}\right) - 4\eta_{iR}\boldsymbol{\varphi}_{iR}^T\boldsymbol{M}\boldsymbol{\varphi}_{iI} + 2\boldsymbol{\varphi}_{iR}^T\boldsymbol{C}\boldsymbol{\varphi}_{iI}$, $p_i = a_i c_i + b_i d_i$, $w_i = b_i c_i - a_i d_i$,

$c_i = \boldsymbol{\varphi}_{iR}^T\boldsymbol{M}\boldsymbol{E}$, $d_i = \boldsymbol{\varphi}_{iI}^T\boldsymbol{M}\boldsymbol{E}$.

STOCHASTIC ANALYSIS

In order to resolve the low calculation efficiency of the conventional stochastic method, Lin proposed a pseudo-excitation method (Lin and Zhang, 2004), in which the seismic random input is converted to be the sinusoidal form to simplify the theoretical derivation and improve the computational efficiency. Firstly, the ground motion is converted into sinusoidal input:

$$\ddot{u}_g(t) = \sqrt{S_{\ddot{u}_g}(\omega)}\mathrm{e}^{r\omega t},\ r = \sqrt{-1}. \tag{11}$$

in which $S_{\ddot{u}_g}(\omega)$ is the power spectral density function. Generally, the method is also applicable for a non-stationary earthquake, and then the power spectral density function varies with time and can be written as $\sqrt{S_{\ddot{u}_g}(\omega,t)}$. Considering the huge computation quantity of the matrix operation, the decoupling computation method utilizing complex mode theory will be introduced in this paper. From derivation above it can be known that the pseudo response of the model described by equation (9) can be written as:

$$q_i = H_i \ddot{u}_g(t) = H_i \sqrt{S_{\ddot{u}_g}(\omega)} \mathrm{e}^{r\omega t} \tag{12}$$

in which $H_i = -\dfrac{1}{\omega_i^2 - \omega^2 + 2r\xi_i\omega_i\omega}$, $i = 1 \sim n+1$. Introducing equation (12) into equation (10), the pseudo response can be obtained:

$$\boldsymbol{U} = \sum_{i=1}^{n+1}\left(\boldsymbol{X}_i q_i + \boldsymbol{Y}_i \dot{q}_i\right) = \left[\sum_{i=1}^{n+1}\left(\boldsymbol{X}_i + r\omega \boldsymbol{Y}_i\right) H_i\right] \sqrt{S_{\ddot{u}_g}(\omega)} \mathrm{e}^{r\omega t} \tag{13}$$

According to the pseudo excitation method, the power spectrum density function matrix of structural response can be expressed as:

$$\boldsymbol{S}_U = \boldsymbol{U}^* \boldsymbol{U}^T \tag{14}$$

If only the lth floor response of the building is concerned (usually the top floor displacement), the pseudo response is given by:

$$u_{sl} = \sum_{i=1}^{n+1}\left(\boldsymbol{X}_{i,l} q_i + \boldsymbol{Y}_{i,l} \dot{q}_i\right) = \left[\sum_{i=1}^{n+1}\left(\boldsymbol{X}_{i,l} + r\omega \boldsymbol{Y}_{i,l}\right) H_i\right] \sqrt{S_{\ddot{u}_g}(\omega)} \mathrm{e}^{r\omega t} \tag{15}$$

in which, $\boldsymbol{X}_{i,l}$ is the lth element of vector $\boldsymbol{X}_i$ and $\boldsymbol{Y}_{i,l}$ is the lth element of vector $\boldsymbol{Y}_i$. Suppose the bridge is supported on the ath floor of building; we can get:

$$u_{b'} = u_b - u_{sa} \tag{16a}$$

$$u_b = \sum_{i=1}^{n+1}\left(\boldsymbol{X}_{i,n+1} q_i + \boldsymbol{Y}_{i,n+1} \dot{q}_i\right) = \left[\sum_{i=1}^{n+1}\left(\boldsymbol{X}_{i,n+1} + r\omega \boldsymbol{Y}_{i,n+1}\right) H_i\right] \sqrt{S_{\ddot{u}_g}(\omega)} \mathrm{e}^{r\omega t} \tag{16b}$$

$$u_{sa} = \sum_{i=1}^{n+1}\left(\boldsymbol{X}_{i,a} q_i + \boldsymbol{Y}_{i,a} \dot{q}_i\right) = \left[\sum_{i=1}^{n+1}\left(\boldsymbol{X}_{i,a} + r\omega \boldsymbol{Y}_{i,a}\right) H_i\right] \sqrt{S_{\ddot{u}_g}(\omega)} \mathrm{e}^{r\omega t} \tag{16c}$$

in which, $\boldsymbol{X}_{i,n+1}$ and $\boldsymbol{X}_{i,a}$ are the $(n+1)$th and ath element of vector $\boldsymbol{X}_i$, $\boldsymbol{Y}_{i,n+1}$ and $\boldsymbol{Y}_{i,a}$ are the $(n+1)$th and ath element of vector $\boldsymbol{Y}_i$, respectively. The control indexes of the integrated building-bridge station in the earthquake are: $\boldsymbol{u}_{control} = [u_{sl}, \ldots, u_{sm}, u_{b'}]$, in which u_{sl} and u_{sm} are the lth and mth displacement of building relative to the ground respectively. In the stochastic analysis, power spectrum density function and square average value are usually adopted, and the square average value can be given as follows:

$$S_{u_l} = u_{sl}^* u_{sl}, \ldots, S_{u_{sm}} = u_{sm}^* u_{sm} \quad , \quad S_{u_{b'}} = u_{b'}^* u_{b'} \tag{17a}$$

$$\sigma_{u_{sl}}^2 = \int_{-\infty}^{\infty} S_{u_{sl}} d\omega, \ldots, \sigma_{u_{sm}}^2 = \int_{-\infty}^{\infty} S_{u_{sm}} d\omega \quad , \quad \sigma_{u_{b'}}^2 = \int_{-\infty}^{\infty} S_{u_{b'}} d\omega \tag{17b}$$

OPTIMIZATION STRATEGY

Some researchers proposed parameter field optimization strategy (Fang, 2004), and in this paper the strategy is used to achieve an appropriate parameter optimization of the isolation devices in the integrated building-bridge station. Combined with the special structural characteristics, the optimization strategy can be expressed as follows:

$$\Omega = \left\{(\omega_b, \xi_b) \middle| R^1 \big/ \left[R^1\right] \le 1, \ldots, R^s \big/ \left[R^s\right] \le 1, R^{s+1} \big/ \left[R^{s+1}\right] \le 1\right\} \tag{18}$$

in which Ω is the parameter field; (ω_b, ξ_b) are the isolation device parameters which would be optimized; $R^1, \ldots, R^s$ are the response quantities of building which need to be controlled; R^{s+1} is the response quantities of bridge which need to be controlled; $\left[R^1\right], \ldots, \left[R^s\right], \left[R^{s+1}\right]$ are the permissible limits of response quantities. In view of the above, the control indexes are $\boldsymbol{u}_{control} = \left[u_{sl}, \ldots, u_{sm}, u_{b'}\right]$, $R^1 = u_{sl}, \ldots, R^s = u_{sm}, R^{s+1} = u_{b'}$.

NUMERICAL STUDY

In this section, a simple analysis model is used to investigate the derived stochastic calculation expression and to validate the optimization strategy. As shown in Figure 2, the structure model is assumed to be a 4-story building, whose 2nd floor supports the bridge structure. The parameters are set as: $m_{s1} = m_{s2} = m_{s3} = m_{s4} = 4 \times 10^5\,\text{kg}$, $k_{s1} = k_{s2} = k_{s3} = k_{s4} = 1 \times 10^9\,\text{N/m}$. The Rayleigh damping is adopted, and a 5% damping ratio is considered for first and 2nd mode of the structure. From the discussion above, the damping ratio of isolation devices on the bottom of bridge does not need optimization, and the stiffness characteristic $k_b = m_b \omega_b^2$ is the optimization factor. The stochastic model of ground motion, the Kanai-Tajimi model, is adopted here, which can be described as:

$$S_{\ddot{u}_g} = \frac{\omega_g^4 + (2\zeta_g \omega_g \omega)^2}{(\omega_g^2 - \omega^2)^2 + (2\zeta_g \omega_g \omega)^2} S_0 \tag{22}$$

in which $\omega_g = 13.96\text{rad.s}^{-1}$ and $\xi_g = 0.72$ are the circular frequency and damping ratio of soil, which correspond to the site type 1 and classification of the earthquake 3 as has been defined in code GB50011-2001 in China. The seismic intensity is assumed to be $S_0 = 0.0006\text{m/s}^3$.

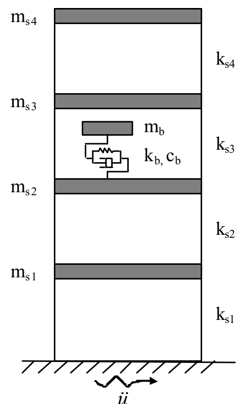

Figure 2. Model of the integrated building-bridge station structure -bridge

Because the vibration control strategy is story isolation, the optimization objective should take into account the lower floor response u_{s2}. First of all, initialize the response of no isolation situation corresponding to the setting that $\xi_b = 0.05$, $\omega_b = \omega_{s1}$, in which ω_{s1} is the circular frequency of first mode of building. Assume the initial response to be $u_{s2,0}$, $u_{s4,0}$ and $u_{b',0}$.The aim of setting isolation devices is not only to reduce the response of the building but also to reduce the response of the bridge. As the damping ratio is assumed to be $\xi_b = 0.2$, the parameter ω_b changing, and the normalized optimization index then can be written as: $\bar{\boldsymbol{u}}_{control} = \left[u_{s2}/u_{s2,0}, u_{s4}/u_{s4,0}, u_{b'}/u_{b',0}\right]$.

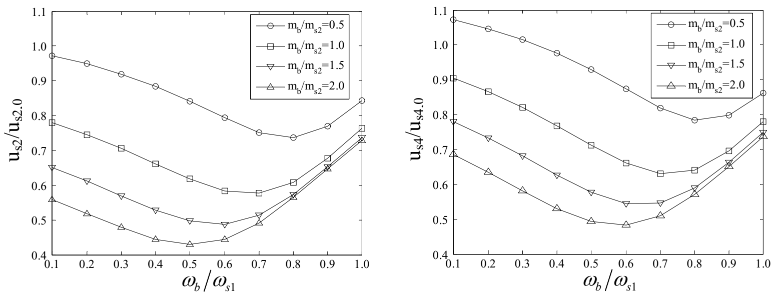

(a) 2th floor (b) 4th floor

FIG.3. Effect of stiffness characteristic of isolation devices on the relative displacement of structure

Figure 3 shows variety of responses of building with changing of the parameters of the isolation devices, from which it can be seen that in order to reduce the response of building the parameters of isolation devices should be appropriate set. Also it shows that there exists an optimal value of stiffness characteristic. Moreover, the effect of vibration control is obviously better as the mass of the bridge increases. However, the work mechanism of the large mass tuned mass damper (TMD), which depends mainly on the damping force but also upon turning frequency, is different from the small mass TMD. Just as is shown in the Figure 3, the optimal frequency will deviate from the turning frequency with the increase of mass of bridge, and the optimal region of stiffness characteristic distributes as $0.4\omega_{s1} \sim 0.8\omega_{s1}$.

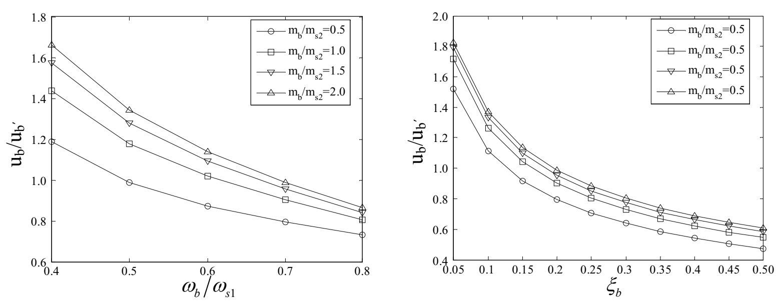

(a) change of stiffness ($\xi_b = 0.2$) (b) change of damping ($\omega_b/\omega_{s1} = 0.7$)

FIG.4. Effect of stiffness and damping characteristics of isolation devices on the displacement of bridge relative to structure

Figure 4 gives the response variation of the bridge along with the change of stiffness and damping characteristics of isolation devices. Figure 4(a) shows that while the damping ratio of isolation devices remains stable, the response of the bridge relative to the building would increase as the stiffness decreases, the change trend of